Received: 12 January 2022 | Accepted: 4 February 2022

DOI: 10.1002/pat.5641

SHORT COMMUNICATION

polymers advanced technologies WILEY

Melt electrowriting to produce microfiber fragments

Hannah Haag[1,2,3] | David Sonnleitner[4] | Gregor Lang[4] | Paul D. Dalton[1,5]

[1]Department of Functional Materials in Medicine and Dentistry and Bavarian Polymer Institute, University Hospital of Würzburg, Würzburg, Germany

[2]Surface and Interface Engineered Materials, Campus Group T, KU Leuven, Leuven, Belgium

[3]Prometheus, Division of Skeletal Tissue Engineering, KU Leuven, Leuven, Belgium

[4]Biopolymer Processing Group, University of Bayreuth, Bayreuth, Germany

[5]Phil and Penny Knight Campus for Accelerating Scientific Impact, University of Oregon, Eugene, Oregon

Correspondence

Gregor Lang, Biopolymer Processing Group, University of Bayreuth, Ludwig-Thomas-Str. 36a, Bayreuth 95447, Germany.
Email: gregor.lang@uni-bayreuth.de

Paul D. Dalton, Department of Functional Materials in Medicine and Dentistry and Bavarian Polymer Institute, University Hospital of Würzburg, Pleicherwall 2, Würzburg 97070, Germany.
Email: pdalton@uoregon.edu

Funding information

Deutsche Forschungsgemeinschaft, Grant/Award Number: 326998133—TRR 225

KEYWORDS: electrohydrodynamic, melt electrospinning writing, polycaprolactone, three-dimensional printing

When using medical-grade poly(ε-caprolactone) (PCL) for melt electrowriting (MEW), one notable feature is that the deposited fiber is typically continuous.[1] Even when the collector speed is increased to 165 mm/s, the direct-written jet is only further stretched but rarely breaks.[2] Such fast speeds were recently taken advantage of to suspend MEW fibers over millimeter wide gaps without sagging[3] in order to form well-defined oriented fiber arrays for neurons.[4]

However, there are several applications where discontinuous microfibers with defined morphology are relevant including the reinforcement of hydrogels in the field of bioprinting, or the use as injectables for drug delivery. Short fibers can induce biological functionality by generating anisotropy,[5,6] improve printability of extrusion-based bioinks[7–10] or alter the mechanical properties of three-dimensional (3D) printed constructs[11,12] while still enabling simple processing through a cannula. Recently the high-speed formation of PCL-dumbbell-like morphologies via precise parametrization of solution electrospinning was demonstrated.[13] Entropy elastic forces in the deposited, not fully dried fibers were found to induce polymer creep which resulted in fiber breakage. The molecular weight of PCL was identified as a critical parameter to tailor the aspect ratio of such fibers in a restricted window.

In this study a MEW process was conducted to produce fragmented microfibers with perfect control on fiber length and without the need of organic solvents. A 20 μm deep microrelief substrate was fabricated with microscopic air gaps and was placed upon an aluminum collector for MEW (Figure 1A). The ambient conditions could be controlled to a level where defined microfiber fragments could be produced. Therefore an elevated temperature environment of 36°C and 60% humidity was used to favor the breakage of the molten jet.

Figure 1B is a photograph of the fragmented fibers on the microrelief substrate, while a top view perspective is provided in Figure S1. In a related study that suspended MEW fibers, a lower temperature of 19.7°C enabled multi-millimeter spanning of fiber walls, while at 23.7°C fibers tended to sag and collapse across air gaps.[3] Here, we increase the ambient temperature to above 36°C, to the level that the molten jet breaks apart due to Plateau–Rayleigh instabilities in the air gap instead of sagging or spanning. Figure 1C shows the approximate polymer melt and ambient temperatures that decide the jet breaking probability.

Interestingly, a slower collector speed slightly above the critical translation speed (CTS) favored jet breaking to form fiber fragments. Figure 1D shows that more fiber fragments were obtained for a collector speed of 1.2 × CTS, while the sample printed with 2.0 × CTS showed suspended rather than broken fibers (Figure 1E and Figure S2). Such breaking at lower collector speeds can be partly attributed to the decreased overall distance that the jet travels to the collector which reduces cooling time[1] and partly due to the latent

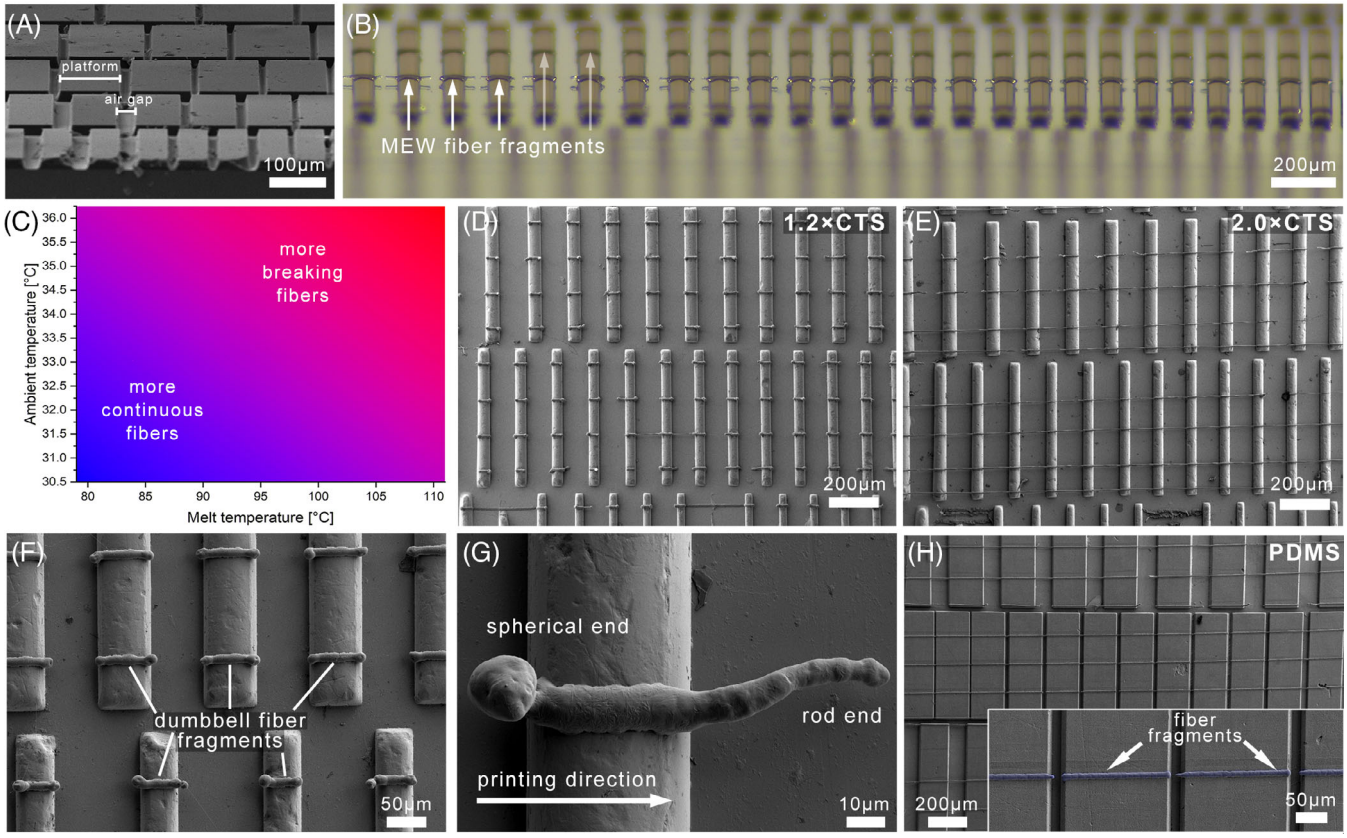

FIGURE 1 (A) SEM image of a microrelief substrate with different air gaps and platform dimensions. (B) Photograph of the MEW fiber fragments that result from direct writing on the microrelief substrate at 33 and 120°C melt temperature. (C) Scheme showing combinations of polymer melt and ambient temperatures that resulted in more, or less, jet breaking. (D) SEM images of MEW fibers produced at 1.2 × CTS, and (E) 2.0 × CTS. (F) SEM images of "dumbbell" fragments produced by using increased air gaps. (G) Fiber fragments with asymmetric shapes in printing direction. (H) A similar breaking effect on microreliefs made from PDMS

heat of a larger jet diameter and therefore a higher mass of melt, sustaining the viscous behavior that is required for breaking.[2]

Using the smallest air-gap achievable (20 µm), the MEW fiber could still be broken at 1.2 × CTS (Figure S3) on the microrelief substrate. The fragment length was primarily defined by the platform width, which ranged from 15 µm up to 80 µm, with greater lengths achievable. The distance between the adjacent fibers does not seem to have an effect on the breakage.

The fiber fragments have different morphologies due to breaking effects. When the air gap is small, the fiber fragment has an abrupt ending; by printing across larger air gaps, a dumbbell-shaped fragment (Figure 1F) would occur. These dumbbell fragments are a result of the broken fiber still being in a molten state and contracting into spheres where it solidifies. Larger gaps result in increased diameter of the spherical end since there is more material in the gap available for the contraction.

The dumbbell-like morphology shown here is similar to another approach that uses solution electrospinning.[13] The driving forces of the fragmentation, elastic forces and intrinsic entropy of the polymer chains, consequently counterbalance within such highly anisotropic stretching of the jet or deposited fiber, irrespective whether it is a polymer solution or melt. Moreover, fiber breaking requires sufficient contact of the fibers on a substrate to avoid sliding and restrict homogeneous shrinkage as previously shown for thermally-induced shape recovery and shrinkage of electrospun regular and chemically crosslinked PCL fibers.[14,15] Another common observation was the occurrence of fiber fragments with a clear spherical front part and an opposing rod-like end, specific to the direct-writing direction. Furthermore, fiber fragmentation is also observed on a PDMS microrelief substrate (Figure 1E). Further images of fiber fragments are shown in Figures S4–S6.

In summary, MEW onto a microrelief substrate regularly broke the fiber in a controlled manner at lower collector speeds, when the temperature was elevated. This study identified the combination of melt and ambient temperatures required for producing defined fiber fragments with well-tailored monomodal lengths. Working without any organic solvents and at moderate melting temperatures of usually less than 100°C, renders this approach of making fragmented fibers attractive for medical applications that include bioink reinforcement, aligned tissue engineering scaffolds[16] or electroactive fibers.

1 | EXPERIMENTAL SECTION

1.1 | Materials

Medical grade poly(ε-caprolactone) (PCL) (Corbion Inc, Netherlands, PURASORB PC 12, Lot# 1712002224, 05/2018) was used as received and stored as described elsewhere.[1]

1.2 | MEW device and processing parameters

All experiments were performed with a custom-built, climate-controlled MEW printer. This chamber allows the control of both temperature and humidity, controlled from 32 to 36°C and 60% relative humidity respectively. A polymer melt temperature ranged from 80 to 110°C, while the remaining conditions are typical for MEW of PCL.[17] This includes an applied voltage of 6.0 kV, a 25G nozzle, a 3.5 mm collector distance and an applied air pressure of 100 kPa. The CTS for MEW at these ambient and melt temperatures are shown in Figure S7.

1.3 | Fabrication of the microrelief substrate

The dimensions of the microrelief substrate were 1.1 cm × 1.2 cm. A digital mask was used to make a microrelief substrate on a silicon-wafer of various platform widths and air gaps to a z-depth of 20 μm. The wafer was cut into squares and coated with an adhesion promoter monolayer and a positive photo-resin (Microchemicals GmbH, AZ 4562, Germany). Smart print rapid prototyping technology (Smart Force Technologies S.A.S., Smart Print, France) was used to directly lithograph an image with a micrometric resolution. After lithography, a developer (Microchemicals GmbH, AZ 400 K, Germany) was used to dissolve the exposed parts of the photoresist. A separate PDMS chip was produced, fabricated by casting a thin layer of onto the resin chip. After detaching the solidified PDMS layer, the corresponding negative shape of the resin chip is obtained.

1.4 | Imaging

Samples were imaged with a Leica DMS1000 digital microscope, or a Crossbeam 340 SEM (Carl Zeiss Microscopy, Göttingen, Germany) equipped with a Zeiss Gemini column to determine the fiber fragment diameter, length, and morphology. An example of imaging the array to count suspended fibers is shown in Figure S3. Prior to SEM analysis all samples were platinum-coated using a Leica EM ACE600 high vacuum sputter coater. The length of 15 fiber fragments were measured at ambient temperatures of 33 and 34°C, and 90°C melt temperatures. An average and standard deviation of 115.0 and 22.6 μm for 33°C ambient temperature, and 83.7 and 9.2 μm for 34°C ambient temperature, respectively.

ACKNOWLEDGMENTS

This work was supported by the Deutsche Forschungsgemeinschaft (DFG, German Research Foundation)—Project number 326998133—TRR 225 (sub-projects A04 and A07). We appreciate the German Research Foundation (DFG) State Major Instrumentation Program for funding the Zeiss Crossbeam CB 340 SEM (INST 105022/58-1 FUGG). Proof-reading by B. Tandon and I. Liashenko is appreciated. Open access funding enabled and organized by Projekt DEAL.

DATA AVAILABILITY STATEMENT

Data available on request from the authors.

ORCID

Hannah Haag https://orcid.org/0000-0002-4281-2563
David Sonnleitner https://orcid.org/0000-0002-6860-3428
Gregor Lang https://orcid.org/0000-0001-9819-8630
Paul D. Dalton https://orcid.org/0000-0001-9602-4151

REFERENCES

1. Hochleitner G, Youssef A, Hrynevich A, et al. Fibre pulsing during melt electrospinning writing. *BioNanoMaterials*. 2016;17(3):159-171.
2. Hrynevich A, Elci BS, Haigh JN, et al. Dimension-based design of melt electrowritten scaffolds. *Small*. 2018;14(22):e1800232.
3. Hrynevich A, Achenbach P, Jungst T, Brook GA, Dalton PD. Design of suspended melt electrowritten fiber arrays for schwann cell migration and neurite outgrowth. *Macromol Biosci*. 2021;21(7):2000439.
4. Dalton PD, Mey J. Neural interactions with materials. *Front Biosci*. 2009;14:769-795.
5. Kim W, Jang CH, Kim GH. A myoblast-laden collagen bioink with fully aligned au nanowires for muscle-tissue regeneration. *Nano Lett*. 2019;19(12):8612-8620.
6. Omidinia-Anarkoli A, Boesveld S, Tuvshindorj U, Rose JC, Haraszti T, De Laporte L. An injectable hybrid hydrogel with oriented short fibers induces unidirectional growth of functional nerve cells. *Small*. 2017;13(36).
7. Sonnleitner D, Schruefer S, Berglund L, Schubert DW, Lang G. Correlating rheology and printing performance of fiber-reinforced bioinks to assess predictive modelling for biofabrication. *J Mater Res*. 2021;36(19):3821–3832.
8. Jessop ZM, Al-Sabah A, Gao N, et al. Printability of pulp derived crystal, fibril and blend nanocellulose-alginate bioinks for extrusion 3D bioprinting. *Biofabrication*. 2019;11(4).
9. Markstedt K, Mantas A, Tournier I, Avila HM, Hagg D, Gatenholm P. 3D bioprinting human chondrocytes with nanocellulose-alginate bioink for cartilage tissue engineering applications. *Biomacromolecules*. 2015;16(5):1489-1496.
10. Jiang T, Munguia-Lopez JG, Flores-Torres S, Kort-Mascort J, Kinsella JM. Extrusion bioprinting of soft materials: an emerging technique for biological model fabrication. *Appl Phys Rev*. 2019;6(1).
11. Kosik-Koziol A, Costantini M, Bolek T, et al. PLA short sub-micron fiber reinforcement of 3D bioprinted alginate constructs for cartilage regeneration. *Biofabrication*. 2017;9(4).
12. Chen WM, Xu Y, Li YQ, et al. 3D printing electrospinning fiber-reinforced decellularized extracellular matrix for cartilage regeneration. *Chem Eng J*. 2020;382.
13. Sonnleitner D, Schäfer N, Wieland A, et al. PCL micro-dumbbells – a new class of polymeric particles reveals morphological biofunctionality. *Appl Mater Today*. 2021;24.
14. Gong T, Li WB, Chen HM, Wang L, Shao SJ, Zhou SB. Remotely actuated shape memory effect of electrospun composite nanofibers. *Acta Biomater*. 2012;8(3):1248-1259.
15. Gao Y, Sim K, Yan X, Jiang J, Xie JW, Yu CJ. Thermally triggered mechanically destructive electronics based on electrospun poly(epsilon-caprolactone) nanofibrous polymer films. *Sci Rep-UK*. 2017;7.
16. Omidinia-Anarkoli A, Ephraim JW, Rimal R, De Laporte L. Hierarchical fibrous guiding cues at different scales influence linear neurite extension. *Acta Biomater*. 2020;113:350-359.

17. Robinson TM, Hutmacher DW, Dalton PD. The next frontier in melt electrospinning: taming the jet. *Adv Funct Mater*. 2019;29(44):1904664.

SUPPORTING INFORMATION

Additional supporting information may be found in the online version of the article at the publisher's website.

How to cite this article: Haag H, Sonnleitner D, Lang G, Dalton PD. Melt electrowriting to produce microfiber fragments. *Polym Adv Technol*. 2022;33(6):1989-1992. doi:10.1002/pat.5641